A Numerical Study of the Terrain Effects on a Squall Line

CHING-SEN CHEN
Institute of Atmospheric Physics
National Central University, Chung-Li, Taiwan, R.O.C.

(Received 27 March 1990; revised 4, May 1990)

ABSTRACT

Observations indicate that some squall line systems moving from the Taiwan Strait towards the mountains would decrease in intensity and dissipate. Obviously the terrain effects on the squall lines are very important. A two-dimensional terrain following coordinated cloud model was used to study geographical effects on a squall line. In the model the mountain peak was assumed to be 1 or 2 *km* in height with the squall line forming over the plain area and propagating towards the mountains. In the plain area new convection continually formed on the forward side of the squall line so that the squall line could maintain itself. When the squall line moved over mountainous areas it slowed down and began decreasing its intensity due to the weakness of new convection. The decrease in intensity resulted from less moisture flowing into the squall line at the higher altitude. The terrain effect on the restriction of the development of the squall line was more evident the higher the mountain.

1. INTRODUCTION

The effects of mountainous terrain on precipitation systems have been discussed very extensively in the past (Smith, 1979). Recently Yoshizaki and Ogura (1988) demonstrated that orographic lifting could induce heavy precipitation in a moisture-rich low-level flow environment. In Taiwan the mountain ranges go north-south-ward and are very lofty, and they can inhibit the development of some precipitation systems propagating eastward from the Taiwan Strait towards the mountains. During TAMEX (Taiwan Area Mesoscale Experiment) a north-south orientated squall line system moved from the strait toward Taiwan island in the late evening of May 16, 1987. It dissipated in the mountainous area the next morning (Cunning, 1988). Another squall line affected by mountains occurred on May 2, 1989. It did some damage in SW Taiwan but decayed when it reached the mountainous area (Chen Wang and Lin, personal

communication). Naturally the question arises as to why the intensity of these squall lines decreased in mountainous areas.

For this paper we artificially formed a squall line using a two-dimensional cloud model in the environment based on a sounding observed at Makung during TAMEX on May 16, 1987. This model squall line was propagated towards the mountains. Investigation of the evolution of the squall line in these mountainous areas will enable us to have better understanding of the influence of terrain on a squall line. This TAMEX case was chosen for use here because Dopplar data were collected for a squall line occurring near mountainous areas. We may thus be able to compare our model result about the topographical effect on the squall line to that in the Doppler analysis after the analysis is finished.

2. THE NUMERICAL MODEL AND INITIAL FIELDS

In order to study the effect of a north-south orientated mountain on a north-south orientated squall line a two-dimensional cloud model was designed. This model was derived from a two-dimensional version of a three-dimensional convective cloud model from Klemp and Wilhelmson (1978). Some modifications have been made: a terrain-following coordinate system was introduced; a wave-absorbing layer was added to the top of the domain; a turbulent mixing parameterization depending on the relative strengths of stratification and shear (Lilly, 1962) was used. The equations used in our two- dimensional model are shown in the Appendix, however a more detailed description of the model is shown in Durran and Klemp (1982).

The terrain structure used in this study is shown in Fig. 1 and the following equation:

$$z_s(x) = \frac{ha^2}{x^2 + a^2}$$

h is the mountain peak and a is 2400 m or 144000 m depending on the x on the west or the east side of the mountain peak, respectively. On the east side of the mountain the altitude decreases more gently than on the west side. This terrain shape is intended to represent the high mountain area on the east part of the domain.

The base of the domain ($z = 0$) and the pressure there are assumed to be 0 m and 1000 hPa, respectively. A warm rain micro- physical parameterization of Kessler (1969) is used, where water is divided into three forms: water vapor, cloud water, and rain. The grid size in the x-direction is constant and is taken to be 1 km, where it is stretched in the vertical to allow finer resolution in the lower atmosphere. There are 361 and 22 grid points in the horizontal and vertical directions, respectively. The model domain is 360 km by 18.2 km. The location of the horizontal velocity u, vertical velocity w, non-dimentional

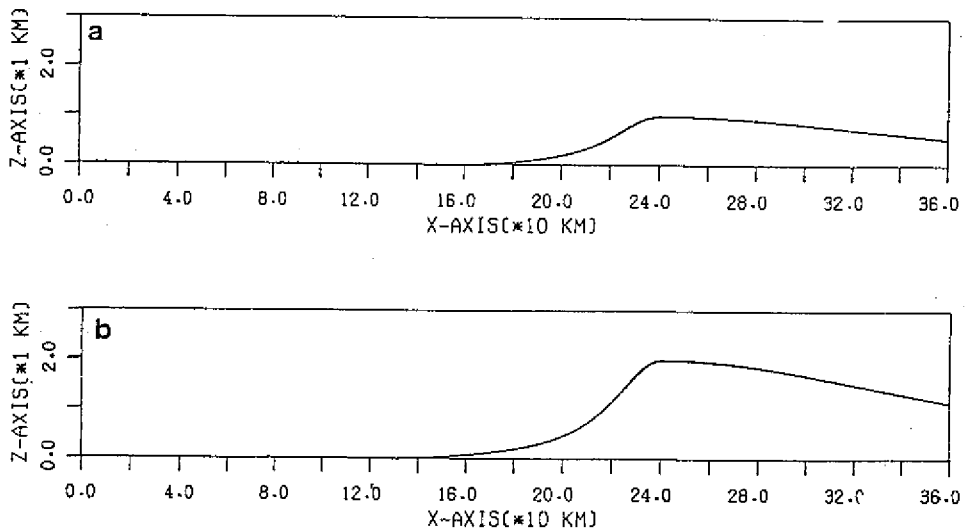

Fig. 1. The terrain features used in run A and B (a) and run C (b).

pressure perturbation π', potential temperature θ, subgrid scale mixing for momentum K_h and scalar K_m, the mixing ratio of water vapor Q_v, cloud water Q_c and rain Q_r in the vertical direction z are shown in Table 1. Their location in the vertical direction η for the terrain following coordinate system is calculated by

$$\eta = \frac{z_t(z - z_s)}{z_t - z_s}$$

where z_t is the top of the domain 18.2 *km*.

Table 1. The location of variables in the z direction. Vertical velocity is located at ZRW position and all other variables are located at ZRT position.

ZRT (m)	ZRW (m)	ZRT (m)	ZRW (m)
18175	18200	5240	4833
16684	17422	4442	4067
15257	15963	3707	3363
13892	14566	3035	2722
12590	13233	2425	2144
11351	11963	1879	1630
10175	10755	1396	1178
9062	9611	975	789
8012	8529	618	463
7025	7511	324	200
6101	6555	92	0
	5663		

Absorbing layers are assumed on the top of the model and are about 11 *km*

thick. Rayleigh damping has been used as in Durran and Klemp (1982).

The initial temperature and moisture conditions for this simulation were based on the sounding taken at Makung at 14 LST on May 16, 1987. It was relatively moist in the troposphere except near 700 hPa (Fig. 2). Based on the temperature and moisture profiles the profiles of potential temperature θ, equivalent potential temperature θ_e, and saturated equivalent potential temperature θ_e^* are presented in Fig. 2b. It was potentially and conditionally unstable below 80 hPa. If an air parcel was lifted from 950 hPa it would acquire a temperature excess beginning at 850 hPa ($\approx 1.5\ km$), the height where its θ_e would exceed the environmental θ_e^*. However if an air parcel was lifted above 900 hPa it would not easily gain positive buoyant energy with respect to environmental θ_e^*.

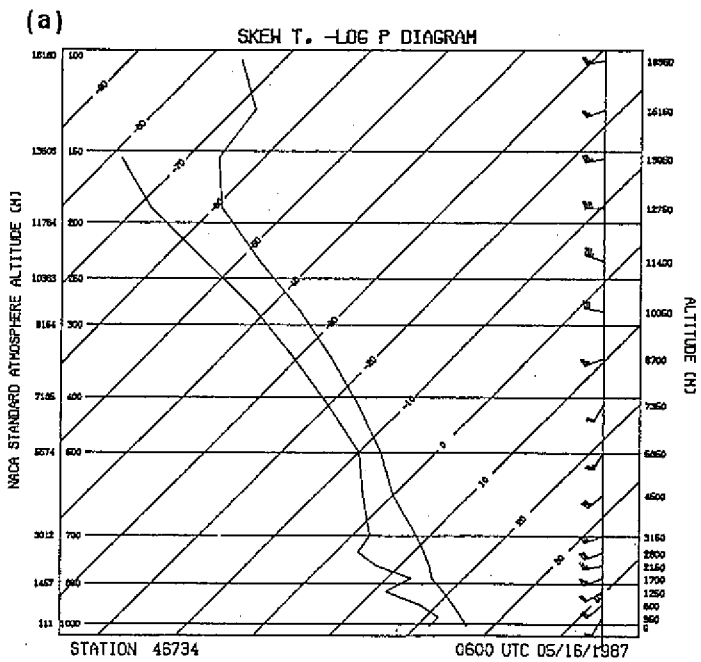

Fig. 2. (a). Initial sounding used in the model simulation taken at Makung at 14 LST, May 16, 1987.

Initially the observed east-west wind component was assigned everywhere in the model above the mountain top. Below the mountain peak wind was gradually increasing over an hour from zero to the observed value of the sounding. Meanwhile all the progonostic variables were integrated forward except cloud and rain. Then we let the model adjust itself by integrating forward without considering any microphysical process for another 11/2 hours.

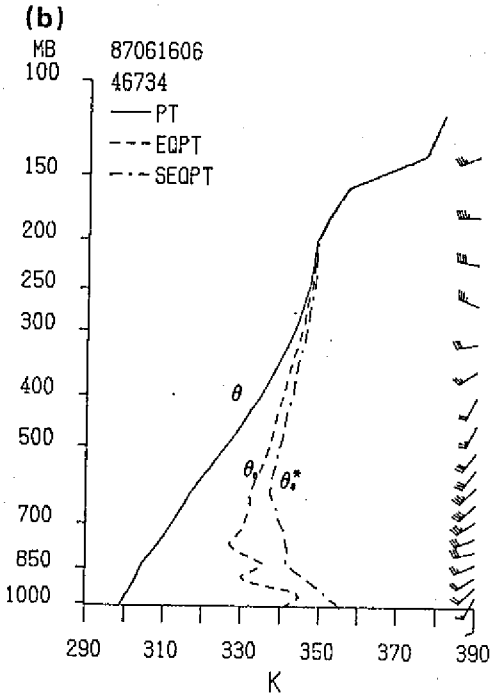

Fig. 2. (b). The profiles of potential temperature θ, equivalent potential temperature θ_e, and saturated equivalent potential temperature θ_e^* derived from *Fig.* 2a.

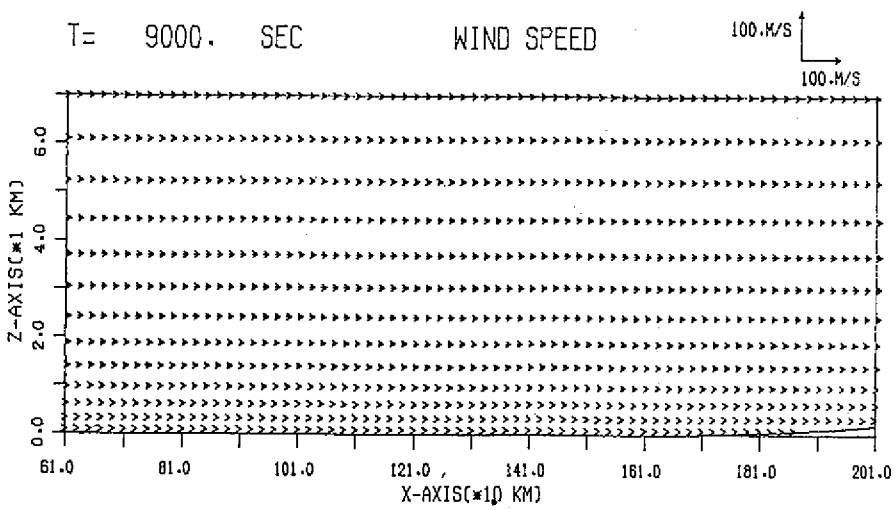

Fig. 3. The flow pattern after the initialization in run A at 9000 *s*. The simulation result is shown in a portion of the domain on every other point horizontally.

At 9000 *s* ($2\frac{1}{2}$ hours) convection was initiated by cooling a region in the low levels 8.0 *km* long by 3.8 *km* thick. This technique was applied to the region located from 60 to 68 *km* away from the left side of the model boundary at a

cooling rate of 0.007 $K\ s^{-1}$ for 10 minutes. Beside that, 10 $g\ kg^{-1}$ of water vapor was added in that region for 10 minutes to accelerate the formation of the precipitation cloud. If the cooling rate was reduced or the magnitude of the extra supply of water vapor was decreased, no precipitation cloud could last longer during our simulation.

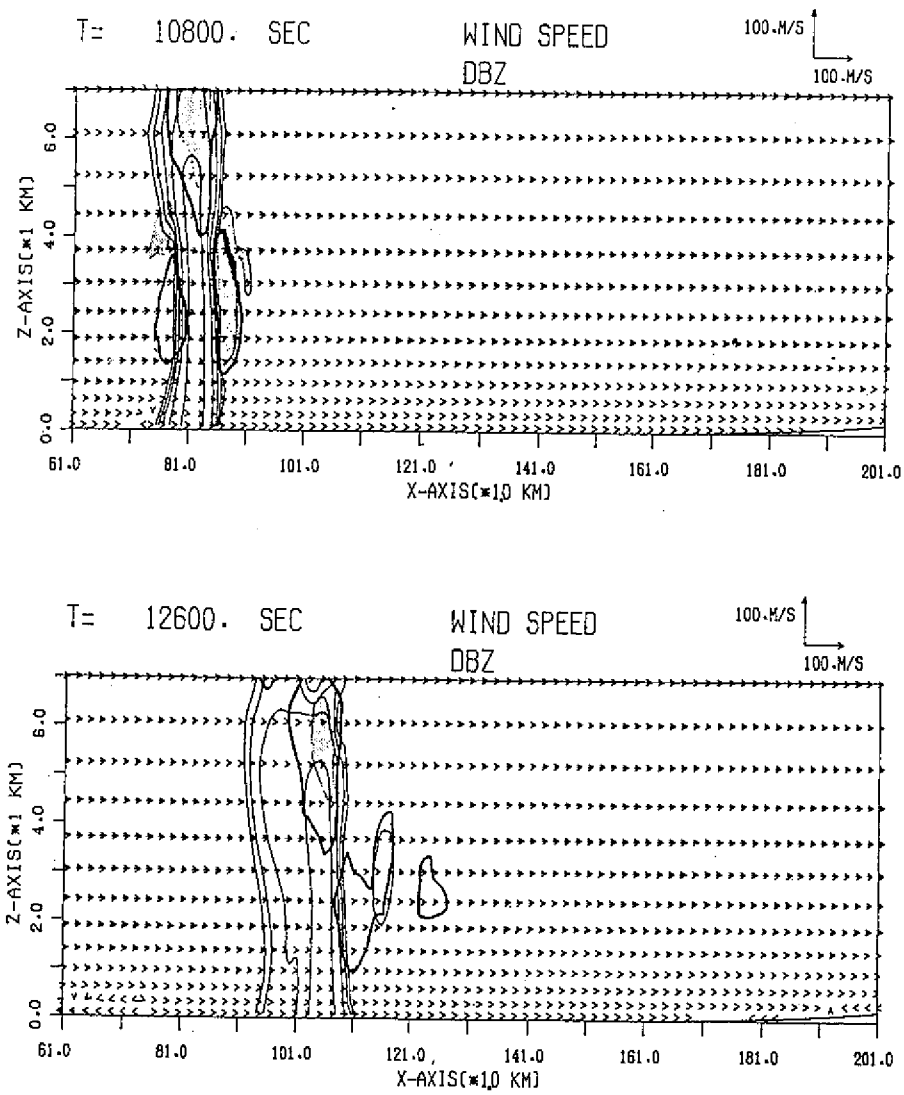

Fig. 4. Model estimated radar reflectivity (dBZ) presented at 30 min intervals from 10800 s to 30600 s in run A on every other point horizontally. The contour intervals are 10 dBZ. Wind vector is superimposed on the reflectivity. The shaded area encloses the vertical velocity greater than 2 $m\ s^{-1}$. The heavy solid line represents 0.1 $g\ kg^{-1}$ the mixing ratio of cloud water.

3. SIMULATION RESULTS

There are three experiments in this study namely, run A, B, C. The terrain features of the three runs are shown in Fig. 1. The mountain top for run A and B is 1 km but 2 km for run C. The difference between run A and run B is that the width of the domain is 300 km for run B but 360 km for A. Since the cooling region that triggers the initial convection is 60 km away from the left side of the domain for run A, B, and C, the initial convection formed in run B was much closer to the mountain.

a. Run A

In order to study topographical effects on a squall line we examined in this experiment the evolution of a model squall line propagating towards the mountains. After initiation of the wind field the flow pattern at 9000 s is shown in Fig. 3 where westerly wind was observed. The simulation results were only presented for a portion of domain in the horizontal and vertical directions, respectively. This implies that simulation results above 7 km in the absorbing layer are not shown here. If no significiantly upward motion existed in the model, no squall line could occur. Therefore we had to artificially supply upward motion to form a squall line. This upward motion would come from some artificial cooling in the low levels. After the artificial cooling and moistening effect applied to the region between $x = 61$ to 68 km in the next 10 min from 9000 s a model sqall line formed near 81 km at 10800 s (Fig. 4). This position was about 160 km away from the mountain peak (at $x = 241$ km). The squall line formed near the leading edge of the cooling air moving toward the the mountain. The intensity of the squall line was represented by the radar reflectivity (dBZ) which was proportional to the mixing ratio of rain (Fovell and Ogura, 1988). The outlines of upward motion (> 2 $m\ s^{-1}$) and cloud (> 0.1 $g\ kg^{-1}$) are superimposed on the dBZ contours. While the model squall line was propagating eastward new convection continually formed on the forward side of the squall line (east side) and the older convection decayed at the back side. The gradient of dBZ was tight near the front edge of the squall line which implied that the convection was strong there. The upward motion was over 2 $m\ s^{-1}$ at the forward side of the squall line as shown in the figures before 19800 s. Before 19800 s the model squall line roughly maintained a speed of 14 $m\ s^{-1}$ towards the east with the maximum intensity over 50 dBZ in the plain area. The magnitude of the westerly wind was reduced on the back of the squall line while it was increased on the leading edge. After 19800 s the squall line climbed the mountain to where the altitude was over 300 m. Less moisture content was observed in Fig. 2 at the higher terrain. The squall line slowed

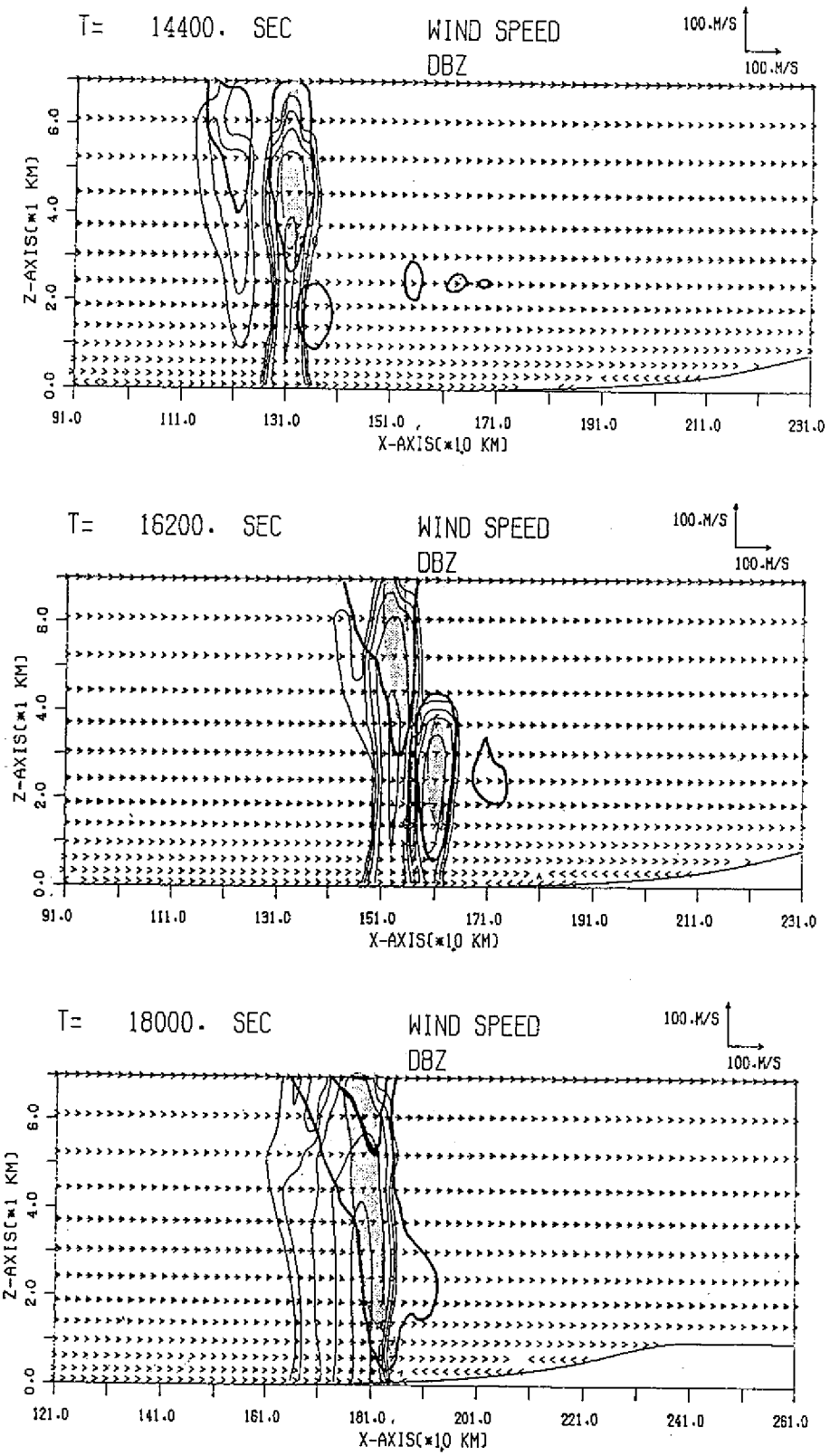

Fig. 4. (Continued)

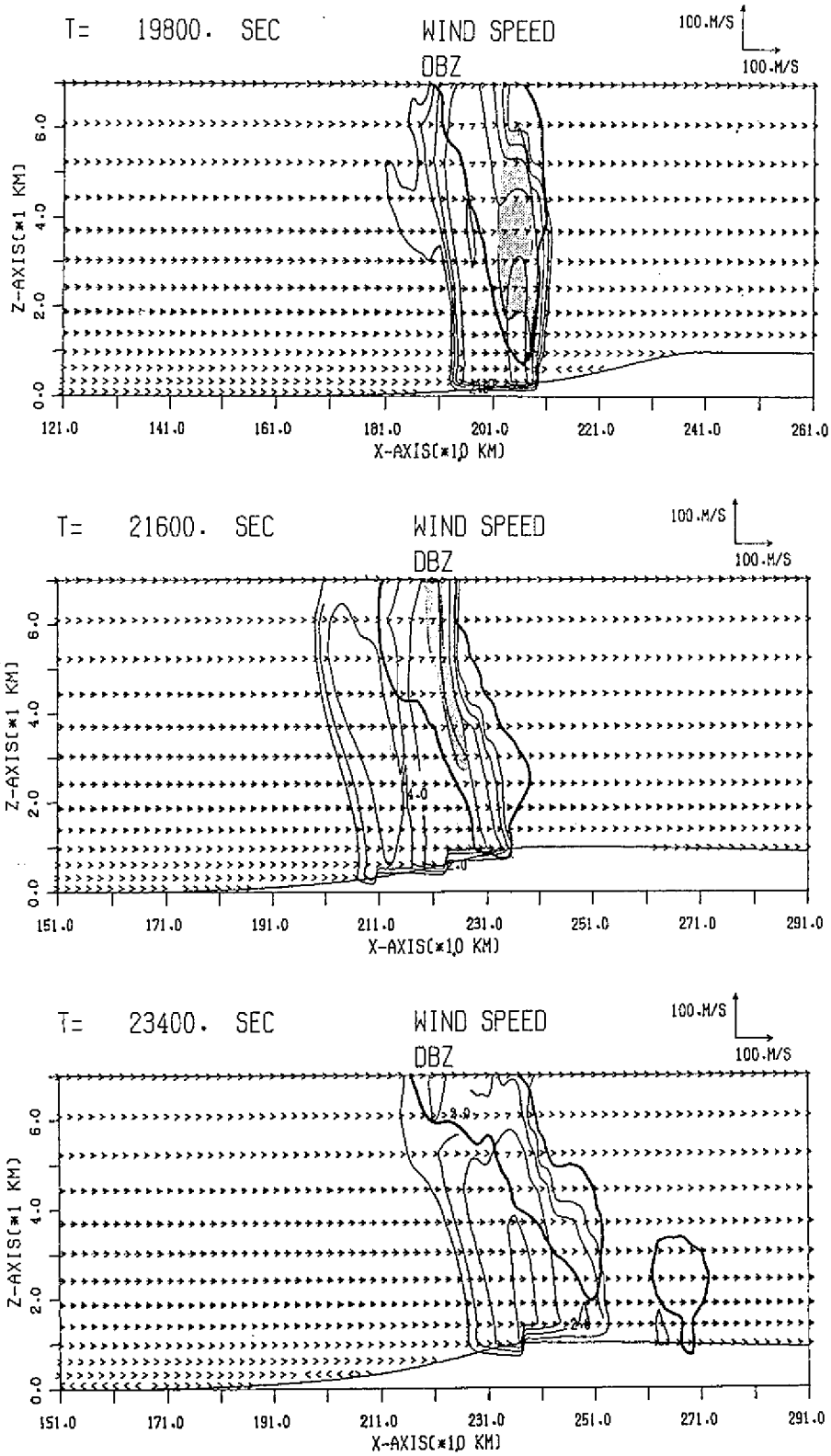

Fig. 4. (Continued)

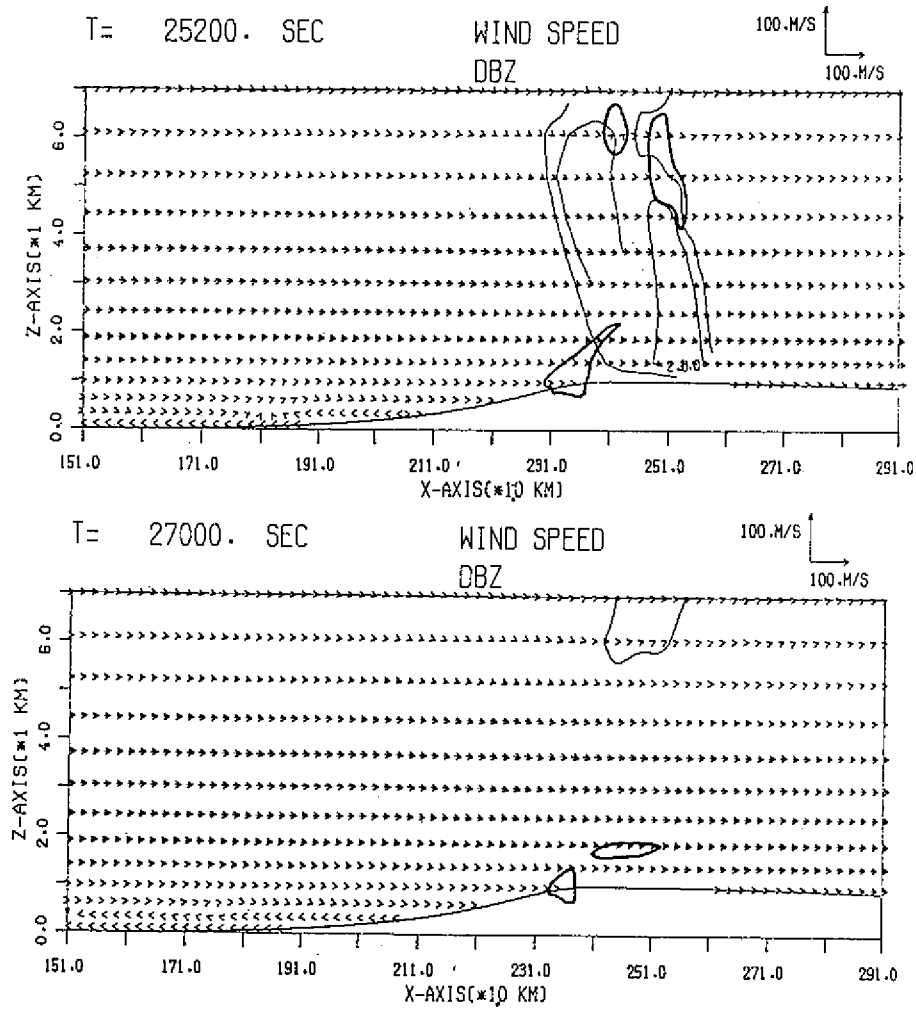

Fig. 4. (Continued)

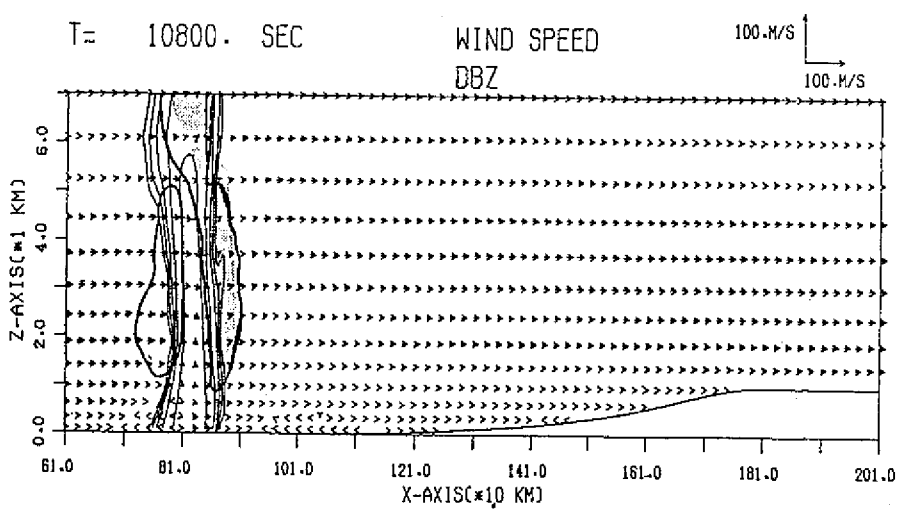

Fig. 5. Same as in *Fig.* 4 but for run B at some selected time.

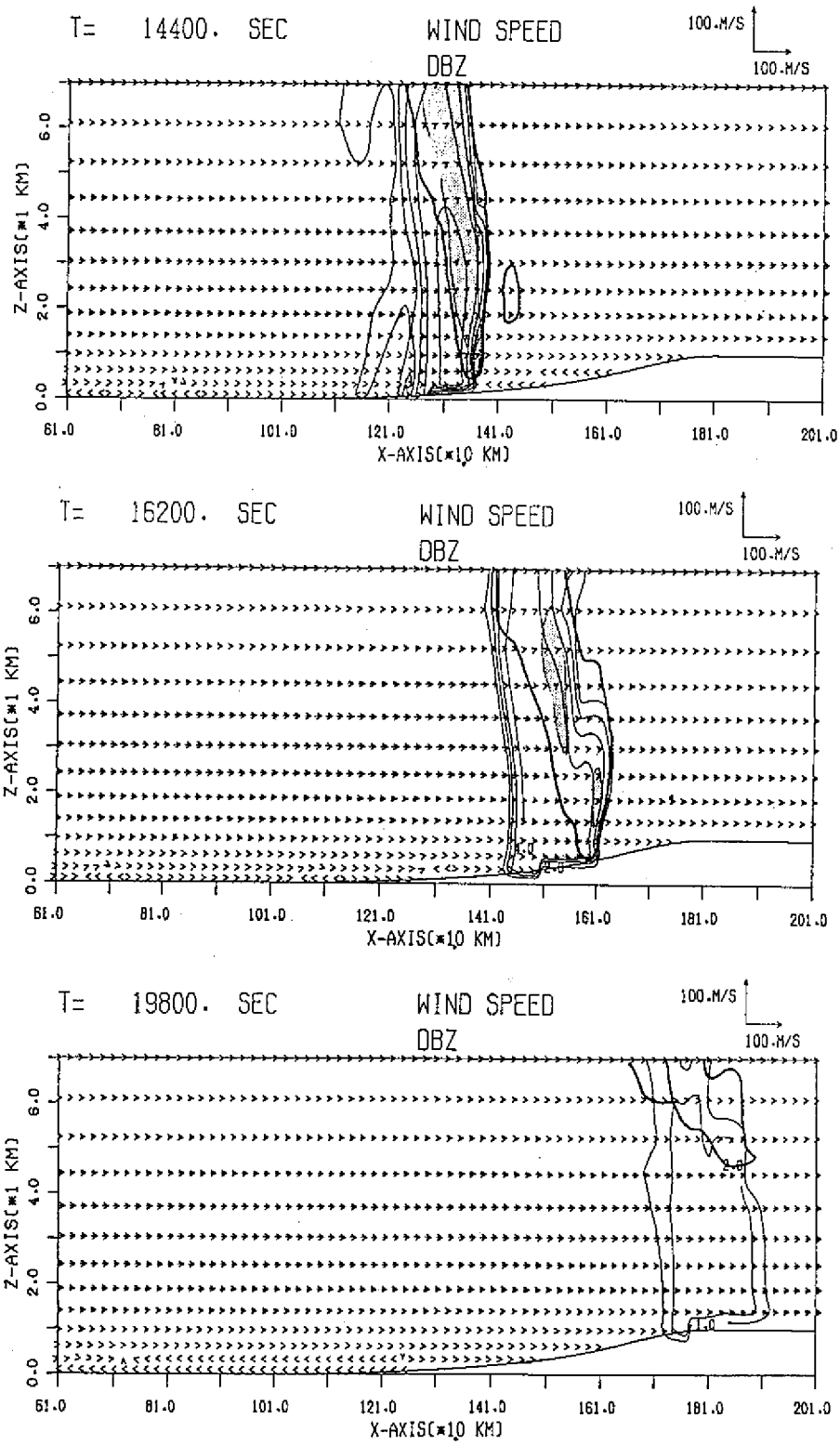

Fig. 5. (Continued)

down and its intensity began decreasing as the new convection on the front side of the squall line weakened as shown in the w pattern. The magnitude of the upward motion was smaller than 2 $m\ s^{-1}$ after 21600 s. This was due to the fact that the moisture flown into the squall line was less in the mountains than that in the plain area. Less moisture supply resulted in less condensation which caused a decrease of the upward motion. As the squall line came over the top of mountain (after 23400 s) it shrank very quickly and dissipated. However some low level clouds could still exist in the mountainous area.

b. Run B

What would happen to a squall line if it formed much closer to a mountain? Run B was set to investigate this phenomenon. Similar initiating procedures to those in run A were used but the coolng and moistening effect to initiate convection at 9000 s was applied to an area much closer to the mountain. Thus a squall line formed much closer to the mountainous area. At 10800 s a squall line (Fig. 4) occurred near 81 km which was about 100 km away from the top of mountain (at $x = 181\ km$). As before this squall line occurred at the front edge of the cooling air moving toward the mountain. Before 14400 s the maximum intensity of the squall line was over 50 dBZ in the plain area. New convection continually formed on the front edge of the squall line to maintain the intensity of the squall line. The magnitude of the upward motion was over 2 $m\ s^{-1}$. After 14400 s this squall line climbed a mountain with an altitude of over 300 m. The intensity of the squall decreased and eventually it dissipated after 19800 s. In the previous experiment the intensity of the squall line was still over 50 dBZ at 19800 s while in this run the intensity was less than 20 dBZ. Both experiments indicated that mountains could inhibit the development of the model squall line when it was in the mountain area no matter how far away from mountain the squall line formed.

c. Run C

This experiment is designed to study the impact of terrain on a squall line moving toward a mountain if its peak is higher (2 km in this run). A similar initiation technique to that used in run A is applied for this experiment. At 10800 s a squall line was found near 81 km about 160 km away from the top of mountain (Fig. 5). Since new convection continually formed on the front edge of the squall line, it could keep its outskirts and its maximum intensity over 50 dBZ untill 18000 s as the squall line moved eastward. Since the lifting due to the mountain was stronger in this run than that in run A, the intensity of the squall line was a little higher in run C before 18000 s as shown in the 50 dBZ

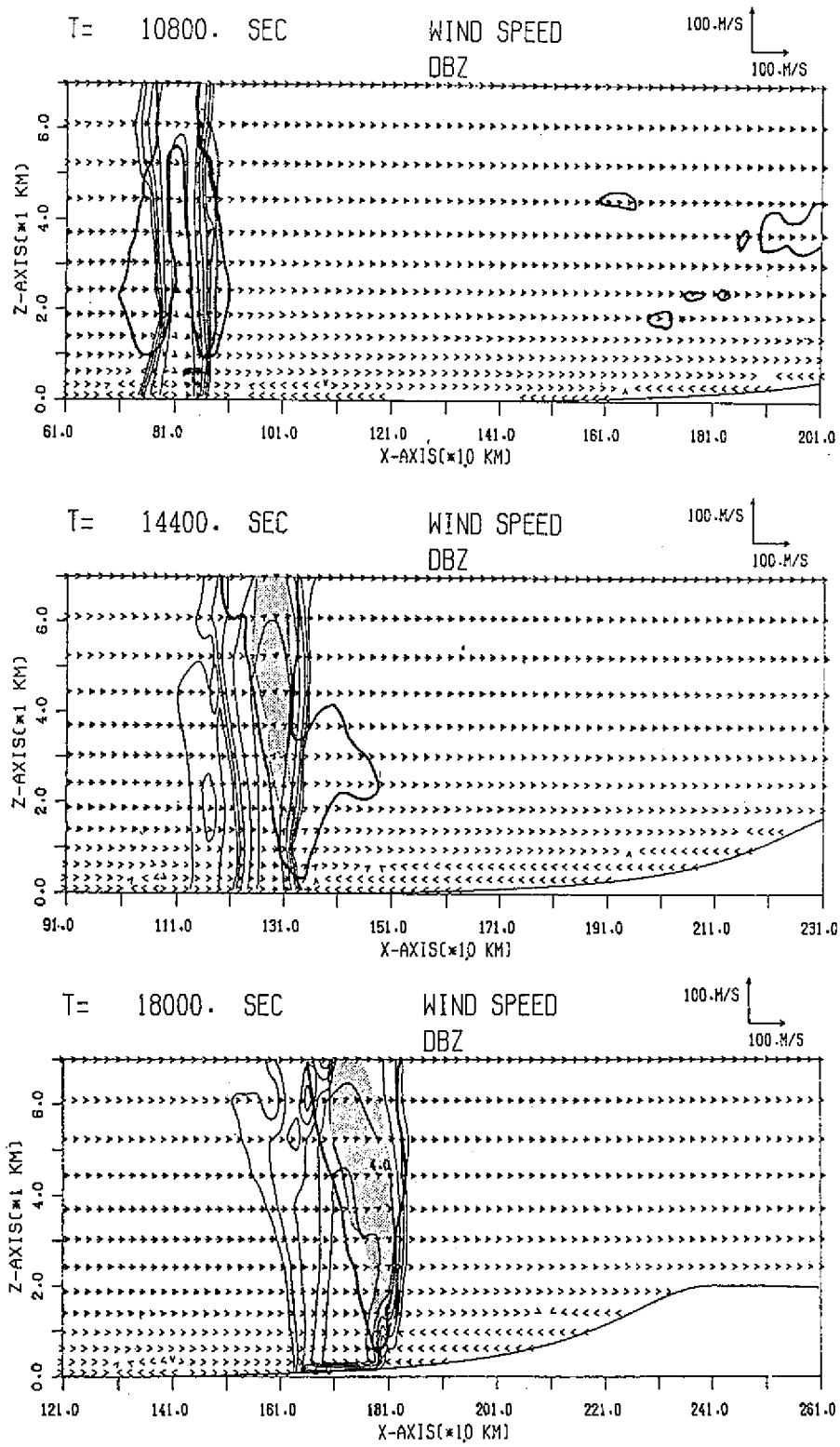

Fig. 6. Same as in *Fig.* 4 but for run C at some selected time.

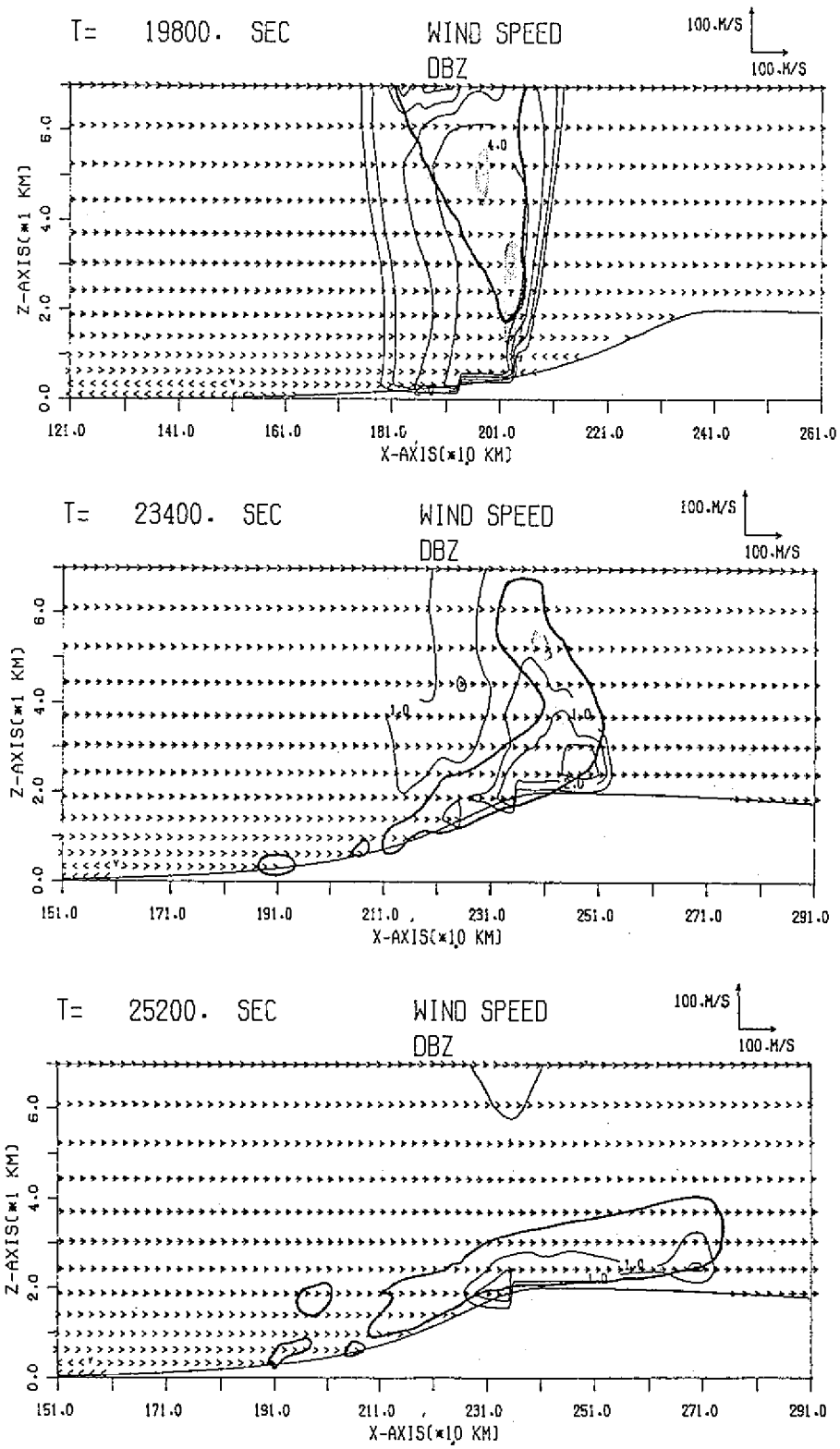

Fig. 6. (Continued)

contour and the upward motion (Figs. 4 and 6). After that the intensity of the squall line began decreasing as it climbed upward above the 300 m height. The magnitude of the upward motion and the radar reflectivity both decreased. As this precipitation system came over the top of mountain precipitation only remained near the ground. The model squall line began to weaken earlier (after 18000 s) than that in run A (after 19800 s) since it encountered higher mountains in run C. The higher the altitude the less moisture supplied to the squall line in the model.

4. CONCLUSION

A two-dimensional terrain following coordinated cloud model was used to study the geographical effect on a model squall line moving toward mountains. The results indicated that a squall line can maintain itself through continual formation of new convection at the front edge of the squall line in a plain area but as the squall line encountered mountains it slowed down and began weakening as a result of the weakness of the new convection. The decrease in intensity was due to less moisture flown into the squall line at the higher altitudes. If the mountain peak was higher, the terrain effects on the inhibition of the development of the squall line was more evident.

Acknowledgments. This research was supported by the National Science Council under grant NSC79-0202-M008-27. I wish to thank Institute of Atmospheric Physics, National Central University for the use of its computer facilities.

APPENDIX

The momentum, thermodynamic, continuity equations and microphysical processes used in this study for the terrain following coordinated system are

$$\frac{\partial u}{\partial t} + u\frac{\partial u}{\partial x} + (Gu + Hw)\frac{\partial w}{\partial \eta} + C_p\bar{\theta}_v\left(\frac{\partial \bar{u}}{\partial x} + G\frac{\partial \bar{u}}{\partial \eta}\right) = D_u$$

$$\frac{\partial w}{\partial t} + u\frac{\partial w}{\partial x} + (Gu + Hw)\frac{\partial w}{\partial \eta} + C_p\frac{\bar{\theta}_v H\partial \pi}{\partial \eta}$$

$$= g\left[\frac{\theta}{\bar{\theta}} - 1 + 0.61(q_v - \bar{q}_v) - q_c - q_r\right] + D_w$$

$$\frac{\partial \pi}{\partial t} + u\frac{\partial \pi}{\partial x} + (Gu + Hw)\frac{\partial}{\partial \eta}(\bar{\pi} + \pi) = 0$$

$$\frac{\partial \theta}{\partial t} + u\frac{\partial \theta}{\partial x} + (Gu + Hw)\frac{\partial \theta}{\partial \eta} = M_\theta + D_\theta$$

$$\frac{\partial q_v}{\partial t} + u\frac{\partial q_v}{\partial x} + (Gu + Hw)\frac{\partial q_v}{\partial \eta} = M_{q_v} + D_{q_v}$$

$$\frac{\partial q_c}{\partial t} + u\frac{\partial q_c}{\partial x} + (Gu + Hw)\frac{\partial q_c}{\partial \eta} = M_{q_c} + D_{q_c}$$

$$\frac{\partial q_r}{\partial t} + u\frac{\partial q_r}{\partial x} + (Gu + Hw)\frac{\partial q_r}{\partial \eta} = M_{q_r} + D_{q_r}$$

where

$$\eta = \frac{z_t(z - z_s)}{(z_t - z_s)}$$

z_t is the top of domain (18.2 km).

$$z_s(x) = \frac{ha^2}{(x^2 + a^2)}$$

h is the mountain peak and a is 2400 m or 144000 m depending on the x in the west or the east side of the mountain peak, respectively.

$$G = \frac{\partial \eta}{\partial x}$$

$$H = \frac{\partial \eta}{\partial z}$$

$$\theta_v = \theta(1 + 0.61 q_v)$$

$$\pi = (\frac{p}{p_0})^{\frac{R}{C_p}}$$

D_u, D_w, D_θ, D_{q_v}, D_{q_c} and D_{q_r} represent the subgrid scale mixing for u, w, potential temperature θ, mixing ratio of water vapor q_v, mixing ratio of cloud water q_c, and mixing ratio of rain water q_r. They all are taken from Lilly (1962) and the mixing coefficient was dependent on the relative strengths of stratification and shear. M_θ, M_{q_v}, M_{q_c}, and M_{q_r} denote the microphysical terms associated with warm rain processes for potential temperature, water vapor, cloud water and rain, respectively. (Klemp and Wilhelmson). Bars over individual variables refers to the initial undisturbed state.

REFERENCES

Cunning, J. B.,1988: Taiwan Area Mesoscale Experiment: Daily operations summary. NCAR Technical Note, NCAR-TN-305+STR, 360pp.

Durrain, D. R., and J. B. Klemp, 1982: The effect of moisture on trapped mountain lee waves. *J. Atmos. Sci.*, **39**, 2490–2506.

Fovell, R. G., and Y. Ogura, 1988: Numerical simulation of a midlatitude squall line in two dimensions. *J. Atmos. Sci.*, **45**, 3846–3879.

Kessler, E., 1969: On the distribution and continuity of water substance in atmospheric circulation. *Met. Mon. Amer. Met. Soc.*, **10**, 84pp.

Klemp, J., and R. Wilhelmson, 1978: The simulation of three-dimensional convective storm dynamics. *J. Atmos. Sci.*, **35**, 1070–1096.

Lilly, D. K., 1962: On the numerical simulation of buoyant convection. *Tellus*, **14**, 148–172.

Simth, R. B., 1979: The influence of mountains on the atmosphere. *Advances in Geophysics*, **21**, 87–230.

Yoshizaki M., and Y. Ogura, 1988: Two- and three-dimensional modeling studies of the Big Thompson storm. *J. Atmos. Sci.*, **45**, 3700–3722.

地形對颱線影響的數值研究

陳景森

國立中央大學大氣物理研究所

摘　要

觀測顯示有一些降水系統如颱線從台灣海峽東移到台灣山區，會受到地形的影響而減低其強度，然後消散。顯然地形效應相當重要，吾人利用一有地形座標的雲雨模式來探討地形對颱線的影響，在模式內，山頂假設1或2公里高，模式中的颱線在平原產生後，能繼續發展。這是因爲在颱線前緣能繼續不斷地產生新生對流併入颱線，維持颱線的強度，但是等到颱線進入山區，移動速度減慢，而且強度減弱，減弱的原因，是由於新生對流變弱，而新生對流的強度衰退，是由於在山區流入颱線的水汽減少。另外模擬結果顯示山的高度愈高，抑制颱線發展的效應也愈大。